Frontiers in Health Informatics www.healthinformaticsjournal.com
ISSN-Online: 2676-7104
2024; Vol 13: Issue 4 Open Access

Interaction studies of Insulin Degrading Enzyme (IDE) with a model membrane

***Shatha R. Zaidan[1],**
Shatha.r@kmc.uobaghdad.edu.iq
***Julia J. Schüer[2],**
Shuer.j@uni-marburg.de

*equally contributed to this work.

1) Institute of Bio-organic Chemistry, University of Saarland, Campus Saarbrucken, 66123 Saarbrucken, Germany

2) Department of Pharmaceutics and Biopharmaceutics, University of Marburg, Robert-Koch-Str. 4, 35037 Marburg, Germany

Cite this paper as: Shatha R. Zaidan, Julia J. Schüer, (2024) Interaction studies of Insulin Degrading Enzyme (IDE) with a model membrane .*Frontiers in Health Informatics, 13* (4), 757-774

Abstract:
Alzheimer's disease is a progressive neurodegenerative disease. A hall mark of AD is accumulation of Aβ peptide. Insulin degrading enzyme IDE has a key role in degrading Aβ intracellularly and extracellularly. It is a zinc metalloendopeptidase and it degrades a wide range of substrates include insulin, amylin, insulin-like growth factors. Cholesterol is an essential component of mammalian bilayer's function and organization. Because of its structure, it can increase the order within the membrane and hence affects membrane fluidity. Although cholesterol has shown modulating effect on IDE by upregulation of its activity, level, stability and gene expression. However, binding between cholesterol and IDE need to be considered. First, binding has been investigated by co-immunoprecipitation and mass spectrometry technique, then were studied with the Langmuir film balance technique. Finally, molecular modelling has been employed with the swissdock. Recombinant human IDE was incubated with cholesterol and co-immunoprecipitated and fed to mass spectrometer to detect the interaction. However, results showed no binding detected. In line with this result, *in-silico* study and Langmuir monolayer assay showed that IDE did not destroy the model membrane.

Introduction

Enhancing beta-amyloid degradation events is the target of several studies to suppress the deleterious impact of the peptide's accumulation (Zaidan, 2020). Participation of cholesterol in the process of Aβ clearance have been studied recently and shown that cholesterol may regulate Aβ degrading enzymes (Wong et al., 2014). One of such enzymes is IDE which transported (after synthesis) to the cell membrane by the secretory pathway and then, it either remains there or is secreted (Wong et al., 2014). Lipid rafts are the domains where IDE is localized (Bulloj et al., 2008). IDE is a thiol zinc metalloendopeptidase (110 kDA) located in the cytosol, peroxisomes, endosomes, and on the cell surface (Saido and Leissring, 2012). Furthermore, degrading activity of several cell lines have been screened, results revealed that IDE participated as a major degrading enzyme of Aβ (Qiu et al., 1998). Cholesterol is an essential ingredient of cell membranes in mammalians. It can increase order within the membrane and thereby affect membrane fluidity, especially in lipid rafts (Grimm et al. 2013). Cholesterol is localized in sizable levels in the brain, where it comprises 25% of the total body cholesterol (Dietschy and Turkey, 2004; Dietschy, 2009; Bjorkhem, 2006) at a content of 15-30 mg/g tissue in the brain whereas in other tissues, the content is 2-3 mg/g tissue (Petrov et al, 2016). Impact of cholesterol have been proven to enhance the enzymatic activity of IDE to degrade Aβ in N2a cells (Zaidan, 2020). In addition, cholesterol proved to increase IDE gene expression, protein level, stability, and activity (Zaidan, 2020). Such impact suggests a

potential interaction between the enzyme and cholesterol which is the interest of the current study. Co-immunoprecipitation is a technique that have been used to identify relevant protein-protein interactions by using antibodies that targeting a protein that is bound or interact with another protein. Then it can quantify and identify binding by proteomics, through utilizing mass spectrometry (Mett 2017). *In-silico* studies showed that the central aromatic residue defined by CRAC (*cholesterol recognition amino acid consensus*) algorithm appeared highly critical for cholesterol binding with proteins in modeling studies (Fantini et al., 2016; Fantini et al., 2013). The CRAC sequence has been suggested to relate to the propensity of membrane proteins to be incorporated into cholesterol-rich lipid domains (Di Scala et al., 2018; Baier et al., 2011).
Also, on a Langmuir film balance, lipids viz. phospholipids can be spread as a membrane model. They assemble at the air/aqueous interface to develop a monolayer called Langmuir film. By compressing and expanding two barriers, the total area of the surface can be varied. By decreasing the area, the surface pressure will increase due to the change in the arrangement of phospholipids on the surface which now have a smaller area per molecule. By injecting a sample like plasmids or peptides in the hydrophilic phase, the interaction with the monolayer can be studied (Christ et. al, 2007 and Oberle et. al, 2000). If there is an interaction, it can be seen as a change in the surface pressure or the area per molecule (Knobler et. al, 1992; McConnell and Harden, 1991, and Mohwald, 1990).

To study the interactions of Insulin Degrading Enzyme (IDE) with membranes, an elementary model was needed. DPPC and cholesterol were used for this purpose. DPPC (1,2-dipalmitoyl-sn-glycero-3-phosphocholine) is the main component of biological membranes and cholesterol is used for stability and fluidity of the membrane (Kent et. al., 1974). Finally, *in-silico* study was performed for the same purpose using Protein Data Bank (PDB) and Swissdock model for the determination of expected binding sites of cholesterol and IDE.

Materials and methods
DPPC and cholesterol were purchased from Avanti Polar Lipids (>99%). The substances were dissolved in chloroform (≥99.8 %, Sigma Aldrich, St.Louis, Missouri, USA) to final concentration of 1 mg/mL. The peptide IDE (>95 %, EC 3.4.24.56, novoprotein, Summit, USA) was suspended in buffer solution (MilliQ®water, 20 mM TrisHCl, 150 mM NaCl, 0.05 % Brij35, 10 % Glycerol, pH 7.5) to 0.6 mg/mL and diluted with Type I water to a final concentration of 10 µg/mL. Type I water from a the Purelab flex 4 apparatus (ELGA LabWater, High Wycombe, UK) with a specific resistance of 18.2 MΩcm was used.

Co-immunoprecipitation
Preparation of sample for detection by mass spectrometer was carried out by preparation of required buffers as follows:Buffer B: IDE assay buffer without inhibitor:100mM,Tris / HCl pH 7.5, 50mM Nacl, 10µM ZnCl2, in ddH2O, Buffer C: wash buffer, 10 mM Tris / HCl pH 7.5 in ddH2O, Recombinant human IDE was incubated with cholesterol by adding 50ng IDE in 200 µl IDE assay buffer B with cholesterol (100 µM) in small glass bottle, for 15 min. at 37 ºC and 300 RPM, and another glass bottle but without IDE, as a negative control, was prepared by the same manner. Centrifugation for 5 min. at 13000 xg and 4 ºC by using Amicon ultra filter tubes, 30 kDa cut-off molecular weight, to separate supernatant that contain IDE (110 kDa) from excess cholesterol. Washing of these supernatants with 200 µl wash buffer C for five times at 13000 xg and 4◦C for 5 min. through filter tube. Transferring 25 µl of supernatant from the last washing step to a new Eppendorf tube and diluted with 475 µl IDE assay buffer B (with 20 µl G-Sepharose protein and 1.5 µg of the IDE antibody ST1120). Incubation for 3h at RT in an overhead shaker. Centrifugation for 1 min. at 13000 xg and 4 ºC Discarding supernatant. Washing the precipitates three times with 1 ml wash buffer C (between washing steps, centrifugation for 1 min. at 13000 xg and 4 ºC and discarding supernatant) Removing washing buffer completely by Hamilton-capillary Incubation of precipitates for 5 min. in 180 µl of ethanol at 98 ºC. After co-immunoprecipitation step (previous steps), precipitates were detected by mass spectrometry. Where samples

were placed in 96-well plate and sealed by silicon mat, shaken for 2 min. at 450 RPM, then placed in the pre-cooled auto sampler to 10 ºC.

Mass spectrometry

Electrospray ionization-based mass spectrometric analysis (4000 QTRAP ABSciex) was carried out in combination with a turbo-spray ion source and sorting proteins according to their mass to charge ratio. The detection and evaluation of the data was carried out using the analyst Software 1.5 of AB Sciex. The following settings are selected for the detection of the species:

Curtain gas (CUR): 20 psi; Collision gas: medium; ion spray voltage: 5500V, temperature (TEM): 200 °C; ion source gas 1: 40 psi; ion source gas 2: 50 psi; interface heater (IHE): on; Entrance potential (EP): 10V; collision cell exit potential (CXP): 10V.

Monolayer experiments

π-t isotherms (surface pressure-time isotherms). For the measurement of the surface pressure a film balance (Riegler & Kirstein, Potsdam, Germany; Teflon trough 100 mL total volume and total area of 170 cm^2) with the filter paper Wilhelmy-method was used. The lipids were dissolved in chloroform to final concentration of 1 mg/mL. Type I water with a temperature of 25 °C was used as subphase. 5 min after spreading the lipids on the surface, the total area was reduced to a surface pressure up to 50 mN/m before IDE (1:35000 enzyme:lipid) or buffer was injected into the subphase (Caseli et. al, 2005). After 30 min the surface pressure was stabilised, the barriers expanded with an area enhancement of 20 $Å^2$/molecule*min^{-1}. After 10 min the barriers were compressed with the same velocity to a surface pressure up to 50 mN/m again (Sriyudthsak et. al, 1987).

π isotherms (surface pressure-isotherms). 5 min after lipids were spread, the barriers were compressed with an area reduction of 20 $Å^2$/molecule*$min^{-1}$to a surface pressure up to 50 mN/m. IDE or buffer in different concentration was injected. After 30 min of equilibration, the barriers were expanded. 10 min of rearrangement of the lipids followed. All cycles were recorded by a control unit (Riegler & Kirstein).

Langmuir-Blodgett transfer

For the visualisation of the phase behaviour and the molecular organisation, the films were transferred onto a hydrophilic silica chip. The chip was suspended using a film lift into the monolayer and retracted back with the vertical velocity of 20 mm/min (Schüer et al. 2020).

AFM

To study the surface morphology an actively vibration isolated atomic force microscope (AFM NanoWizard 3, JPK Instruments, Berlin, Germany; on a Halcyonics i4 Vibration damping system, Accurion, Göttingen, Germany), and installed in a JPK Acoustic Enclosure (JPK Instruments) was used. N-Type Silicon tips (HQ:NSC14/Al BS, MicroMasch, Sofia, Bulgaria) were used in Tapping Mode. The resonant frequency was about 140 kHz and the scan speed between 0.5 and 1.0 Hz. To image the sample's surface the amplitude signal of the cantilever, the height signal and the phase signal were used.

Results

Mass spectrometry

Effect of cholesterol on IDE by increasing the enzymatic activity (Zaidan, 2020), points out that may be there is interaction or binding between the enzyme and cholesterol. For this purpose, co-immunoprecipitaion followed by mass spectrometer was carried out to discover binding properties. In addition to the measure of binding by co-immunoprecipitation, Langmuir monolayer method were used as well as in-silico study of cholesterol docking to IDE using Swissdock. Testing of binding by different approaches was carried because,

there was no interaction detected by co-immunoprecipitation and mass spectrometer analysis as shown in Fig. 1.

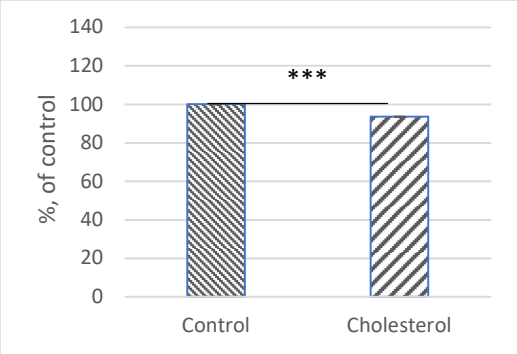

Fig. 1: Interaction study between cholesterol and recombinant IDE.

Incubation time was 15 min. Co-immunoprecipitation followed by mass spectrometry (n=3).
Error bars represent standard deviation of results.

Asterisks show the statistical significance compared to control (*** $p \leq 0.0001$).

π-t isotherms and π-isotherms of the DPPC: Cholesterol (70:30) model without injecting IDE

In figure 2a the π-t isotherm shows the cycles run by observing the surface pressure change. In phase 1 the surface pressure increased because the surface area was reduced by moving the barriers together. Phase 3 shows a decreasing surface pressure because the surface area increased by moving the barriers apart. 4 is an equilibration phase. In phase 2 the barriers stood still and the decreasing surface pressure was caused by a new array of the lipids in the monolayer over time as well as processes like relaxation and desorption takes place (Munden et. al., 1968; Nino et. al., 2008; Ter, 1956).

In figure 2b the area per molecule got smaller by every cycle. The lipids rearranged by every change of the surface area up to the closest position in which they can be and an extrusion of some molecules in the subphase took place (desorption; Munden et. al., 1968; Nino et. al., 2008; Ter, 1956).

a.

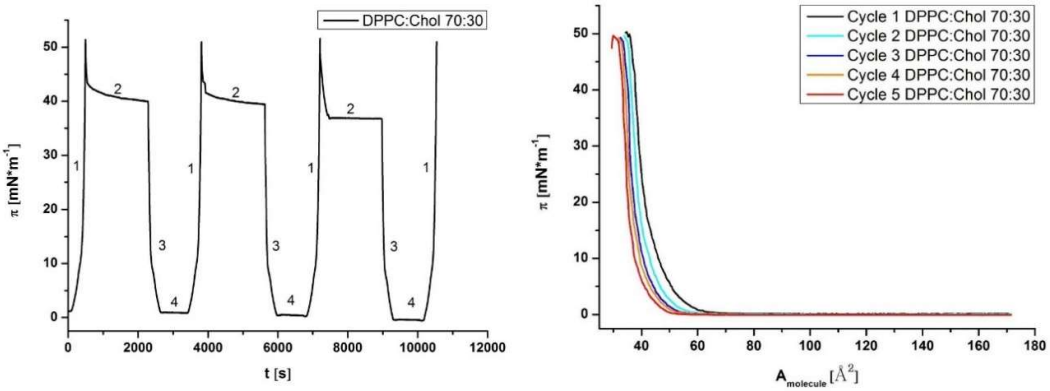

Fig. 2: 11.0 µL of DPPC:Cholesterol (70:30) (1 mg/mL) spread out on a water phase. The surface pressure increased up to 50 mN/m by compressing the barriers with an area reduction of 20 $Å^2$/molecule*min^{-1}. After 30 min of equilibration, the barriers expanded with the same velocity. After 10 min of equilibration, the procedure was repeated.

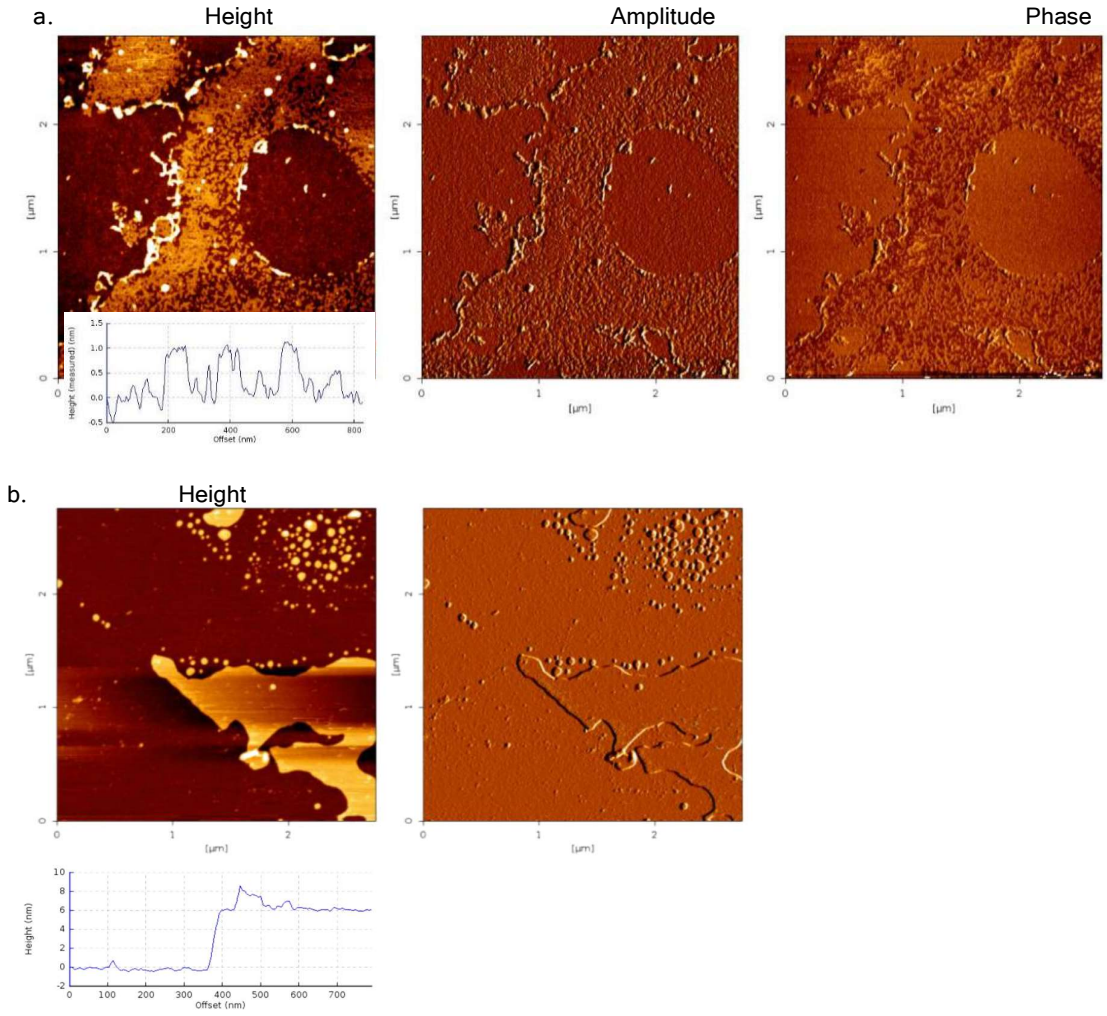

Fig. 3: The lipid monolayer was transferred on to a hydrophilic silica chip and studied using an atomic force microscope.

The film in figure 3a was transferred applying a surface pressure of 5 mN/m. At the surface pressure of 5 mN/m the lipids were in a transition from the gas phase to the liquid expanded phase (Schüer et al. 2020). This is also shown in figure 3b. Every molecule had a molecular area from about 55 $Å^2$. The lipids lay on the chip in the gas phase but also had interactions with each other in the liquid expanded phase. This is shown in the height graph were the lipids had a height of 1 nm by building a non-homogeneous film.

The Film in figure 3b was transferred applying a surface pressure of 40 mN/m after the fifth cycle. At the surface pressure of 40 mN/m the lipids were in the solid condensed phase. This phase was optically continuous. The lipids stood upright with a height of 2.8 nm. There is no flow in the membrane and the compressibility is low as the surface pressure is close to the collapse lim

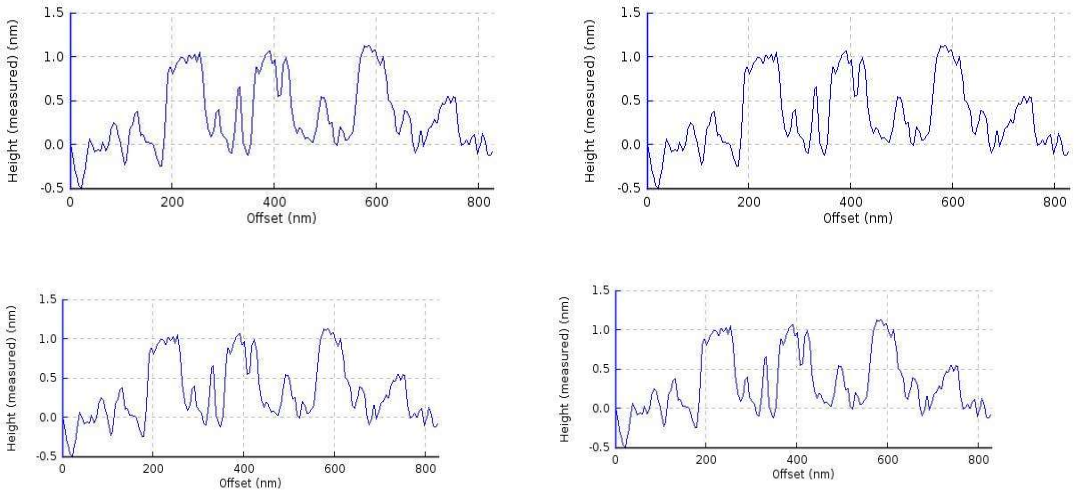

it (seen in Fig. 2b). In the right part of figure 3b some multilayer structures can be found. These structures were justified by desorption of some molecules during the previous cycles (Munden et. al., 1968; Nino et. al., 2008; Ter, 1956).

π-t isotherms and π- isotherms of the DPPC:Cholesterol (70:30) model by injecting the buffer

The buffer in which the enzyme was suspended and stabilised, includes Brij35 (Polyoxyethylen-(23)-laurylether). As a non-ionic surfactant, it assembles at the air/aqueous interface and has surface active properties, which is shown in the following π-isotherm (Fig. 4).

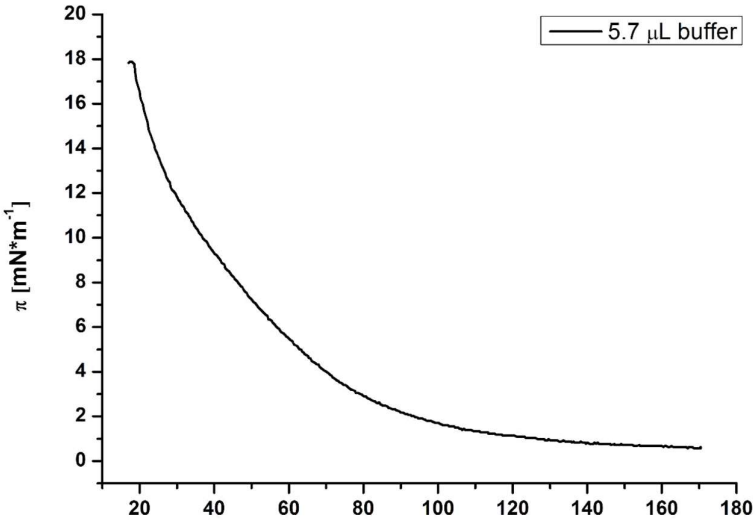

Fig. 4: 5.7 µL of the buffer (MilliQ® water, 20 mM Tris HCl, 150 mM NaCl, 0.05 % Brij35, 10 % Glycerol, pH 7.5) spread out on the water phase. The surface pressure increased up to the collapse by compressing the barriers with an area reduction of 20 Å^2/molecule*min^{-1}

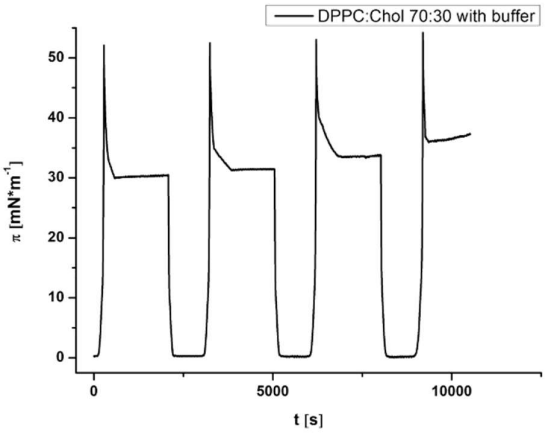

Because of the surface active properties of the buffer, the π-isotherm and the π-t isotherm of the DPPC:Cholesterol (70:30) monolayer had to be studied by injecting the buffer without the enzyme to see if there is an influence on the monolayer. To have a comparison of the results, the volume of injected buffer corresponding to the volume of the enzyme-buffer suspension needed for the enzyme-membrane interaction studies.

Tab. 1: By using the same monolayer of DPPC:Cholesterol (70:30), an increasing volume of the buffer or enzyme-buffer suspension had to be used in every cycle to increase the injected amounts of IDE in total. With every cycle, the amount of Brij35 increases.

Tab. 1 Cycles of increasing buffer and IDE.

Cycle No.	**Injected volume of** buffer or buffer-enzyme suspension per cycle [µL]	**Injected volume of** buffer or buffer-enzyme suspension in total [µL]	**Molecular amount** of IDE injected in total (III.) [pmol]	**Mass of Brij35** injected in total (II.) [µg]
1	5.7	5.7	0.5	$5.64 * 10^{-3}$
2	5.7	11.4	1.0	$11.28 * 10^{-3}$
3	11.4	22.8	2.0	$22.56 * 10^{-3}$
4	34.2	57.0	5.0	$56.40 * 10^{-3}$
5	57.0	114.0	10.0	$112.80 * 10^{-3}$

a.

b.

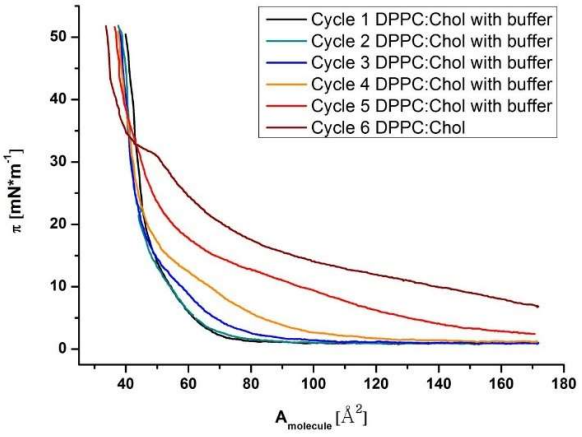

Fig. 5: 11.0 µL of DPPC:Cholesterol (70:30) (1 mg/mL) spread out on the water phase. The surface pressure increased up to 50 mN/m by compressing the barriers with an area reduction of 20 $Å^2$/molecule*min^{-1}. An increasing volume of buffer solution is injected in every cycle. After 30 min of equilibration, the barriers expand with the same velocity. After 10 min of equilibration, the procedure was repeated and the next cycle was initiated.

In figure 5a the π-t isotherm after injecting a volume of buffer corresponding to the volume of the enzyme-buffer suspension (as seen in Tab. 1) is shown. The π-t isotherm shows the cycles run by observing the surface pressure change. The experimental procedure was the same like in figure 2a. After reaching a surface pressure above 50 mN/m the barriers were stopped and the volume of buffer for the first cycle (5.7 µL) was injected. After expansion of the barriers the second cycle is recorded by injecting another 5.7 µL after the barriers were stopped above a surface pressure

about 50 mN/m. In the subphase a total volume of 11.4 µL buffer was located. After the third cycle it was 22.8 µL in total. With every injection the plateau of the cycle stayed on a higher surface pressure.

Figure 5b shows the π-isotherm after injecting a volume of buffer corresponding to the volume of the enzyme-buffer suspension as seen in Tab. 1. For reasons of clarity and comprehensibility the curves were not imaged while expanding the barriers. The π-isotherm shows no obvious differences in the properties in cycle one and two in comparison to the run without buffer. In both cases 5.7 µL buffer were injected in the subphase. No change in the progression and the gradient of the curve can be detected. From the third cycle, the progression of the isotherm changes and from the fourth cycle, an increasing area per molecule can be observed. After injecting 34.2 µL of buffer in the subphase, a sixth cycle with no further injection of the buffer was executed. The progression was modified with a new plateau. A small deviation was observed at 32 mN/m.

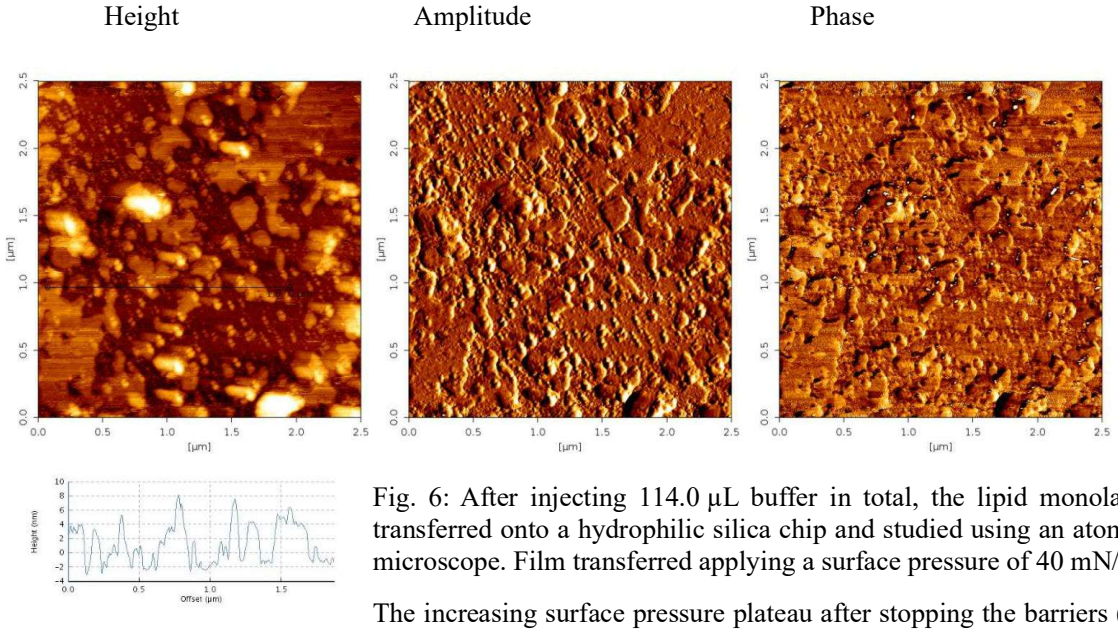

Fig. 6: After injecting 114.0 µL buffer in total, the lipid monolayer was transferred onto a hydrophilic silica chip and studied using an atomic force microscope. Film transferred applying a surface pressure of 40 mN/m.

The increasing surface pressure plateau after stopping the barriers (Fig. 5a) was due to the surface-active substance Brij35 which assembles at the air/aqueous interface between the monolayer of DPPC:Cholesterol (70:30). This causes the increasing plateau surface pressure in figure 5a and the increasing area per molecule in figure 5b. There were more molecules at the air/aqueous interface than before. The applied lipids from the monolayer seem to need more space at the air/aqueous interface but this was accounted by the additional injected surface-active substance. With an increasing amount of Brij35 the progression and the gradient of the curve changed. The monolayer became more flexible because of the molecular structure of Brij35. It did not have the linear structure at the interface as DPPC has, so the packing density of the molecules was lower. The monolayer got more fluidic and less compressible because of the steric difference between the molecules. This is seen in the new plateau by an increasing amount of Brij35 where there was enough time to integrate into the monolayer. The lipids had no more ability to arrange in the new position by an increasing surface pressure because of the different packing. The deviation which is seen in the π-isotherm in figure 5b cycle 6 is an indication of a squeezing out of one of the monolayer's compounds (Schüer et al. 2020a; Goerke, 1998). This hypothesis is confirmed by the multilayer shown in AFM image in figure 6. After cycle 6, a second layer with a height of 6-10 nm was located on top of the first. One of the surface-active substances was squeezed out of the monolayer

Because of the change in the isotherm's progression as higher concentrations of the buffer were injected, novoprotein was contacted. It was possible to dilute the delivered sample with Type I water. The 16.0 µL of

the enzyme-buffer suspension was filled up with MilliQ®water to 1.0 mL. After the dilution with MilliQ®water, the buffer concentration was 60x lower than the concentration in this part of the experiment. Due to the fact that no change in the isotherm's progression in cycle one and two can be detected, a buffer volume under 11.4 µL can be used. The changes caused by higher buffer concentrations did not have to be taken into consideration for the following interaction studies.

π-t isotherms and π-isotherms of the DPPC:Cholesterol (70:30) model by injecting IDE

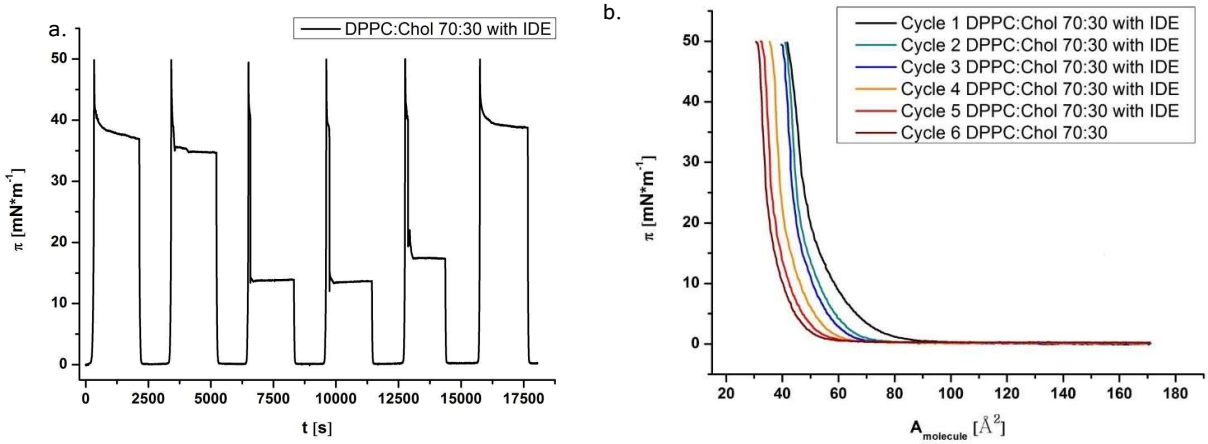

Fig. 7: 11.0 µL of DPPC:Cholesterol (70:30) (1 mg/mL) spread out on a subphase. The surface pressure increased up to 50 mN/m by compressing the barriers with an area reduction of 20 $Å^2$/molecule*min^{-1}. An increasing volume of enzyme-buffer suspension was injected by every cycle. After 30 min of equilibration, the barriers expanded with the same velocity. After 10 min of equilibration, the procedure was repeated and the next cycle was initiated.

The π-t isotherm after injecting a volume of the enzyme-buffer suspension as seen in table 1 is shown in figure 7a. The π-t isotherm shows the cycles run by observing the surface pressure change while injecting IDE after compressing to a surface pressure up to 50 mN/m. In the first cycle 5.7 µL of the enzyme- suspension which corresponds to 0.5 pmol IDE was injected in the subphase. The surface pressure decreased during the following equilibration. The same properties occurred in the second cycle, where another 0.5 pmol enzyme were injected. From the third cycle on, where 11.4 µL suspension was added, the surface pressure decreased to a surface pressure under 14 mN/m. A similar observation can be made in the next two cycles. In the sixth cycle no injection took place. The surface pressure did not fall like it did, when the suspension was injected.

In figure 7b the π-isotherm after injecting a volume of the enzyme-buffer suspension as seen in table 1 is shown. For reasons of clarity and comprehensibility the curves while expanding the barriers were not imaged. The π-isotherm shows the influence on the properties in cycle runs by injecting an IDE solution in increasing amounts into the subphase. The used amounts are shown in table. 1. From the first cycle onwards the area per molecule decreases by every cycle. The progression got sharper.

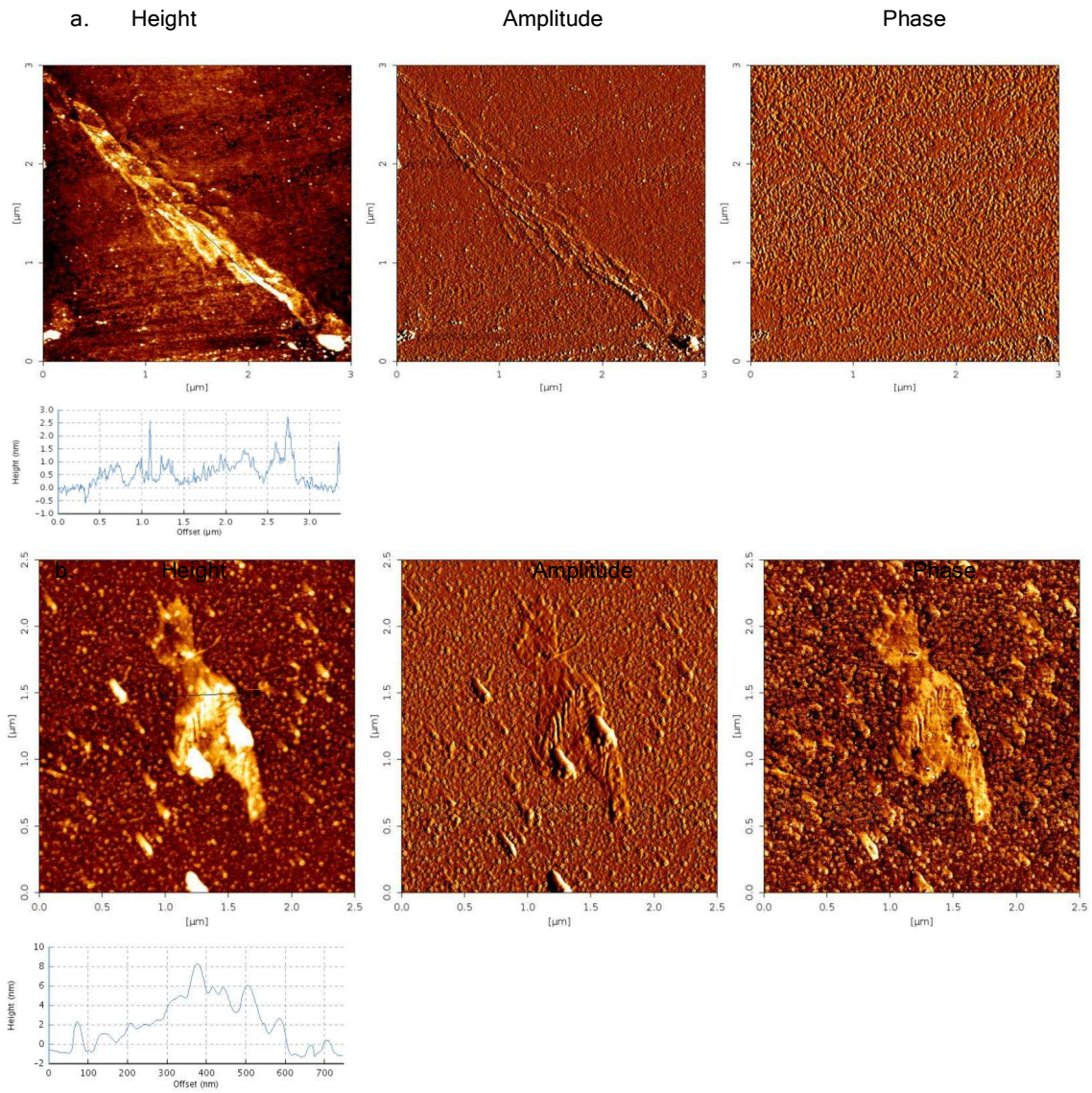

Fig. 8: After the cycles with IDE injection the lipid monolayer was transferred on to a hydrophilic silica chip and studied using an atomic force microscope. (a.) at a surface pressure of 5 mN/m and (b.) at 40 mN/m.

After 24 h, the film was transferred applying a surface pressure of 5 mN/m to see if there was an interaction of the enzymes with the monolayer. This 1 to 2.5 nm high structure in figure 7a could be the residual IDE after 24 h in water at a temperature of 25 °C.

On the silica chip which is transferred after 24 h at the surface pressure of 40 mN/m, also a specific structure can be found (Fig.7b). The height is 8 nm and it is in a different phase than the lipids.

This work shows that IDE did not destroy the model membrane. After a temporary interaction with the lipids, which could be due to the injection of IDE directly under the monolayer, the monolayer could rearrange again. The enzyme is enabled to build vesicles and leave the monolayer at a higher surface pressure. After the leaving of IDE, the isotherm showed no different properties as is had before when no IDE was injected. In the cycles

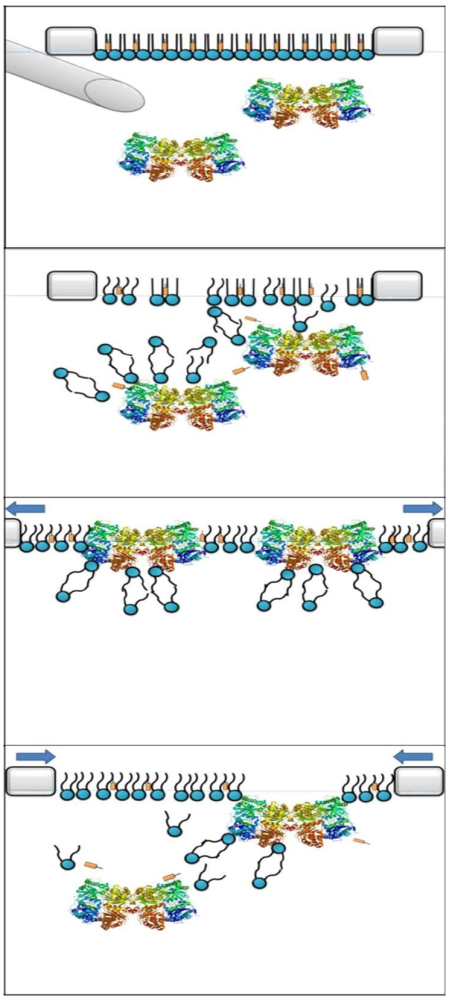

after the last injection of IDE all properties were the same, even after 24 h no difference in the π-t and π-isotherms could be observed.

Fig. 9: After injecting IDE under a compressed monolayer of DPPC: Cholesterol (70:30), the surface pressure decreased because of a spontaneous interaction of IDE with some lipids of the monolayer. After expanding the barriers IDE arranged at the air/aqueous interface. IDE showed no disruption of the monolayer and returned in the hydrophilic sub-phase.

In-silico study of the interaction between cholesterol and IDE

The aim of SwissDocking program was to find the correct binding mode of a ligand. Not to predict affinity. The first run was done in order to detect all potential cholesterol binding sites.

PDB: 4pes, 2.21 Å resolution was used in the process (https://www.rcsb.org/structure/4PES).

Basically, only two potential cholesterol binding areas were detected inside the active site cavity (A and B) as shown in Fig. 10. It should be noted that cholesterol was more frequently predicted to bind in Area A than in B, as seen from the clustering of the superimposed binding poses below.

Further processing: the best ten poses were visually inspected. Among these, poses showing mere surface binding without a visible, concave binding pocket were discarded. The remaining 7 poses were subject to a docking refinement using Chemical Computing Group (MOE) as shown in Fig. 10.

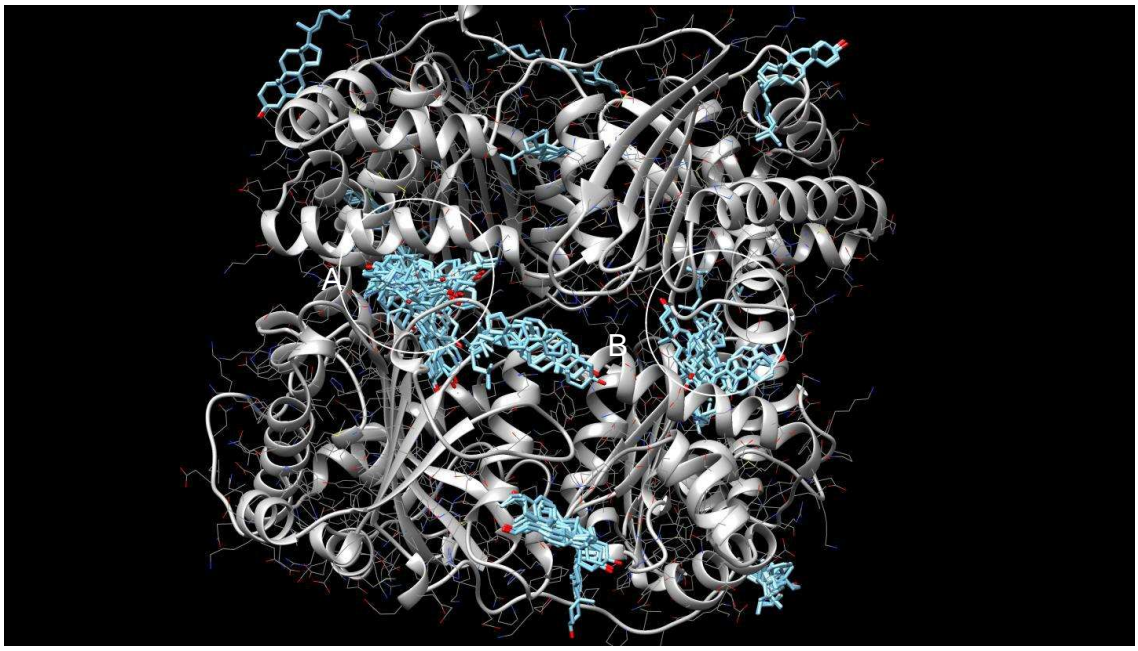

Fig. 10 Potential binding sites between IDE and cholesterol.

Using MOE, the selected poses were re-docked, enabling flexibility of the cholesterol ligand and the side chains of the protein. From the seven selected Swissdock poses, three converged to show a very similar binding mode (Fig. 11). Another binding pose was obtained showing the ligand close to the active site Zn2+ ion, which would most probably lead to an inhibition.

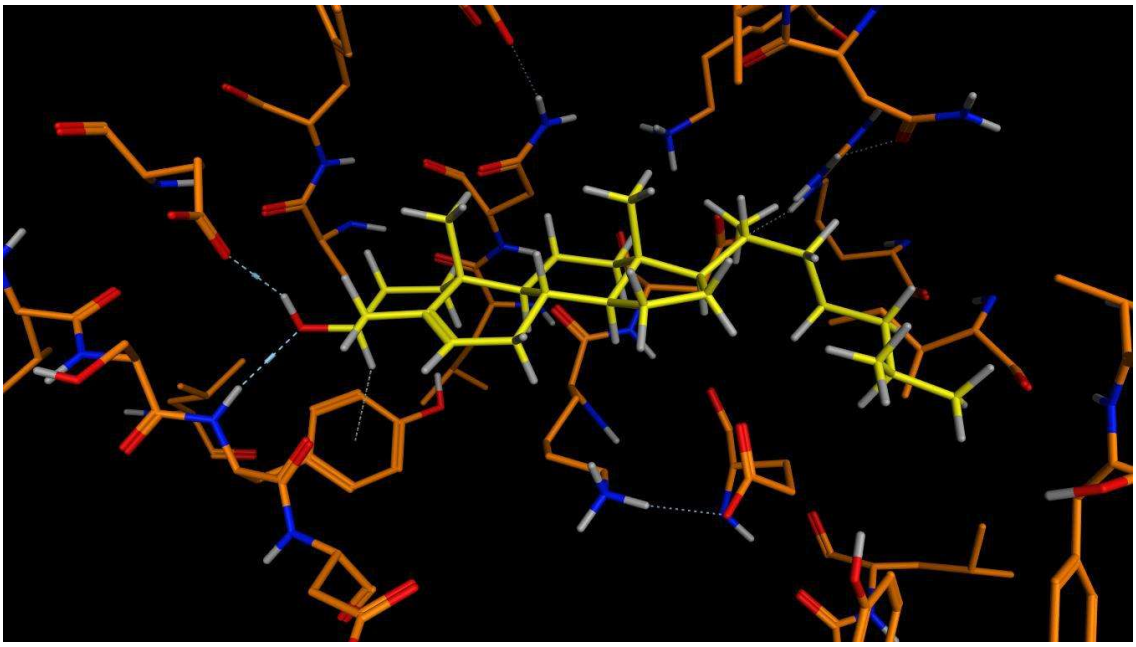

Fig. 11 Binding modes of cholesterol.

All other predicted binding modes were less reasonable, as the ligand was either placed in areas with mainly hydrophilic side chains, or there was no complementary pocket shape.

Finally, only one binding site fulfilled the criteria for a potential cholesterol binding which would not result in enzyme inhibition (Fig. 12). This binding site was inside the enzyme´s cavity in the former region A, showing good shape complementarity to cholesterol, with two hydrophobic areas at both ends. It also featured two H-Bond interactions with the cholesterol OH (important for specific recognition of the molecule) and in some binding modes, an additional CH-π interaction with a phenylalanine side chain. Different superimposed predicted binding modes for cholesterol in the same binding site as on the previous image. Note that the OH group always makes the same H-bond interactions, while the lipophilic skeleton of the cholesterol can be placed over a somewhat larger area. Color codes: blue, hydrophilic; brown: hydrophobic.

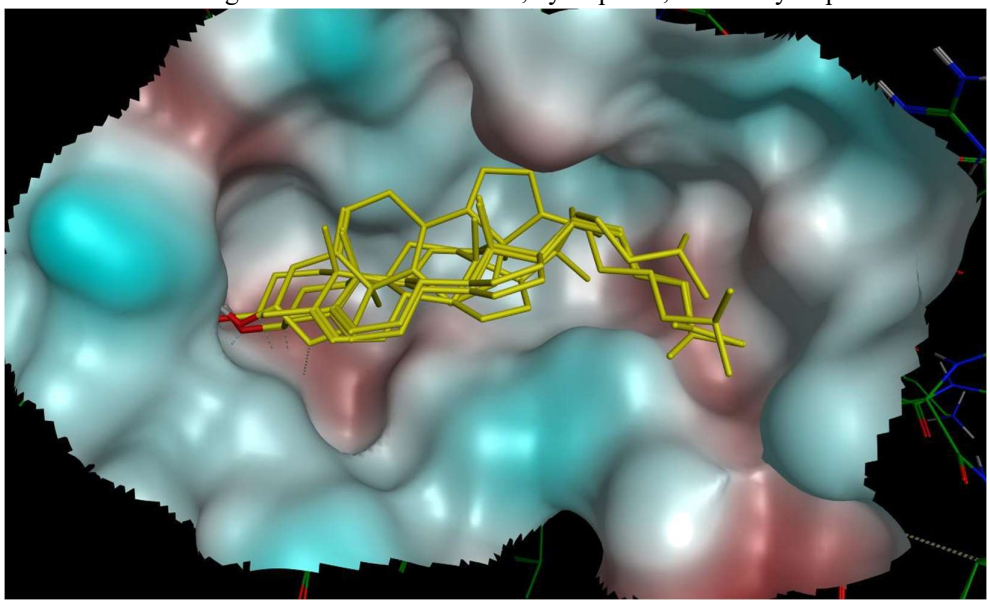

Superimposition of the predicted (Fig. 13) cholesterol (yellow) binding site and the A-beta peptide (magenta) as co-crystallized in PDB entry 4M1C. The active site Zn2+ is also shown as a cyan sphere.

Fig. 12 Predicted binding site of cholesterol to IDE

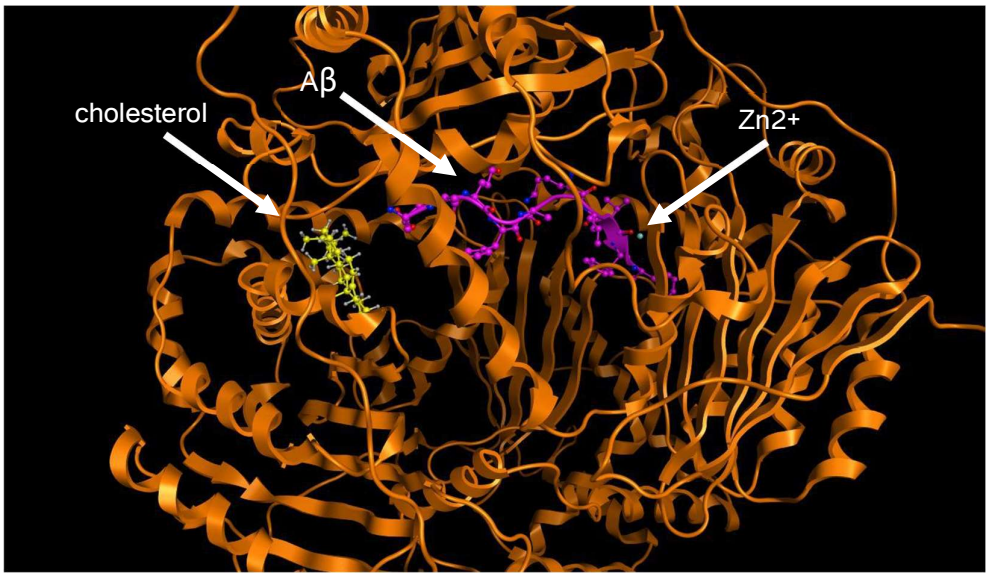

Fig. 13 cholesterol (yellow) binding site and the Abeta peptide (magenta) as co-crystallized in PDB entry 4M1C

Discussion

It has been reported that the multiple proteases are associated with the decrease in amyloid beta aggregation including IDE (Zaidan, 2020), NEP (Mett, 2017; Grimm et al., 2015), endothelin-converting enzymes, and plasmin in the cytosol or cell membrane, and IDE in the extracellular (Weller et al., 2000). IDE degrades the Aβ peptide intracellularly and extracellularly where, IDE is secreted through unconventional pathway (Zhao et al., 2009) or because of the loss of cell integrity (Song et al., 2018). Knocking down the IDE activity in the extracellular side has enhanced Aβ aggregation (Zaidan, 2020). This result confirms the key role of IDE in the process of extracellular catabolism of Aβ (Steffen et. al, 2017; Bright et. al, 2015; and Fung et. al, 2004). However, co-Immunoprecipitation results revealed no interaction was detected between IDE and cholesterol as shown in Fig. 1 (94% ± 11%, $P \leq 0.001$) when compared to control samples that did not contain cholesterol. Likewise, In Fig. 7(a), the reduction of the surface pressure in the equilibration time by every cycle is seen. This reduction was due to the injected IDE. This phenomenon did not appear in the cycle runs without injecting IDE (Fig. 2a). Also, the buffer can be excluded as a reason for this, because the buffer induces an increasing surface pressure in the remaining time (Fig. 5a). The implication is that the injected IDE has an instant interaction with the compounds of the monolayer so that they left the air/aqueous interface in a bigger amount. The surface pressure decreased because less molecules were on the interface at this moment. Also, the fact that the surface pressure in the equilibration time of the sixth cycle (Fig. 7a), where no IDE was injected, did not decrease the way it did in the cycles before, indicates that the reduction of the surface pressure was caused by injecting the IDE.

Figure 7b, shows a decreasing area per molecule by every cycle run. In comparison to the cycle runs of the pure monolayer (Fig. 2b) the progression was flat in the beginning. In surface pressure range among 15 mN/m the enzyme interacted with the lipid monolayer between its hydrophilic and hydrophobic part. With increasing surface pressure, a sharp surge was observed in the progression and the enzyme leaved the monolayer. The area per molecule after 5 cycle runs amounts to 40 $Å^2$ like it did without IDE. The area per molecule decreases by every cycle as stated above because of the rearrangement and exclusion of some molecules into the subphase because of desorption processes (Sriyudthsak et. al., 1988; Munden et. al., 1969; Nino et. al., 2008). Even the cycle runs 9 and 24 h after injecting the enzymes showed no difference in their appearance. There was no wide

variance in the decreased area per molecule as it might be expected after the distinct reduction of the rest-surface pressure during the equilibration time in figure. 7b. this fact indicates that the compounds of the monolayer did not leave the air/aqueous interface permanently because of the interaction with the IDE. The lipids were not constantly linked with the enzymes. After the equilibration time when the barriers drifted apart, the lipids which were in the sub-phase because of the spontaneous interaction with IDE, returned to the air/aqueous interface and integrated into the monolayer again.

Because there was no enhancement of the area per molecule in figure. 4b, it is clearly recognizable that IDE was not integrated permanently into the monolayer (Sriyudthsak et. al., 1987). Instead, it returned into the hydrophilic sub-phase and also directly under the monolayer. This is shown in figure. 8a and 8b. By transferring the monolayer to the silica chip, specific structures can be found which seem to be the residues of IDE.

Although, results of docking showed a probable site of interaction. However, these results cannot be taken into consideration unless confirmed by mass spectrometry and/or Langmuir film balance results.

Conclusion:

Previous studies evidenced the role of cholesterol in increasing the enzymatic activity of IDE to degrade Aβ which suggest a potential interaction may be developed between the enzyme and cholesterol. In the current study, this hypothesis have been studied thoroughly by utilizing mass-spectrometry, Langmuir monolayer film, and *in-silico*. Nevertheless, according to the results acquired through mass-spectrometry experiments no interaction has been detected between the enzyme and cholesterol. Confirmation of this outcome is shown by the un-changed area per molecule of the cholesterol monolayer. Finally, *in-silico* studies suggests weak signs of potential interaction sites which are not supported by *in-vitro* studies.

References:

1. Caseli, L., Rafael, G.O., Douglas, C.M., Furriel, R.P., Francisco, A.L., Bruno, M. and Zaniquelli, E.D. (2005). *Effects of molecular surface packing on the enzymatic activity modulation of an anchord protein on phospholipid Langmuir monolayers*. Langmuir, **21**, 4090-4095.

2. Christ, K,. Imke, W., Bakowsky, U., Hans-Georg S., and Gerd, B. (2007). *The role of lipid II in membrane binding of and pore formation by nisin analyzed by two combined biosensor techniques*. Biochemica et Biophysica Acta 1768, **10** 694-704.

3. Goerke, J. (1998). *Review Pulmonary surfactant: functions and molecular composition*. Biochemica et biophysica acta 1408, **10** 79-89.

4. Kent, C., Schimmel, S.D. and Vagelos, P.R. (1974). *Lipid composition of plasma membranes from developing chick muscle cells in culture*. Biochemica et Biophysica Acta, 360, **9** 312-321.

5. Knobler. Charles M. (1992). *Phase transitions in monolayers*. Annu. Rev. Chem. **43**: 207-36.

6. McConnell, H.M. (1991). *Structures and transitions in lipid monolayers at the air-water interface.* Annu. Rev. Phys. Chem. **42**: 171-95.

7. Mett, Janine. (2017). *Die regulation Aβ-degradierender enzyme durch die interazellulare domane von APP (AICD) und die lipidhomoostase*. Ph.D. thesis, University of Saarland, College of Medicine.

8. Mohwald, H. (1990). *Phospholipid and phospholipid-protein monolayers at the air/water interface*. Annu. Rev. Chem. **41**:441-76.

9. Munden, J.W., Blois, D.W. and Swarbrick, J. (1968). *Surface pressure relaxation and hysteresis in stearic acid monolayers at the air-water interface*. Journal of pharmaceutical sciences, j. appl. Microbiol., **16**, 1102.

10. Nino, M.R., Rodrigues, A.L. and Rodrigues J.M.P. (2008). *Relaxation phenomena in phospholipid monolayers at the air-water interface*. Colloids and surface A: physicochemical and engineering aspects 320.1, **10** 260-270.

11. Oberle, V., Bakowsky, U., Zuhorn, I.S. and Hoekstr, D. (2000). *Lipoplex formation under equilibrium conditions reveals a three- step mechanism*. Biophysical journal vol. 79, **7** 1447-1454.

12. Schüer, J. J., Arndt, A., Wölk, C., Pinnapireddy, S. R., & Bakowsky, U. (2020). Establishment of a synthetic in vitro lung surfactant model for particle interaction studies on a Langmuir film balance. *Langmuir*, *36*(17), 4808-4819.

13. Schüer, J. J., Wölk, C., Bakowsky, U., & Pinnapireddy, S. R. (2020a). Comparison of Tanaka lipid mixture with natural surfactant Alveofact to study *nanoparticle* interactions on Langmuir film balance. Colloids and Surfaces B: Biointerfaces, 188, 110750

14. Sriyudthsak, M. (1987). *Enzyme-immobilized Langmuir-blodgett film for a biosensor*. Third int. conference on Langmuir-Blodgett films, Gottingen, F.R.G., **5** 26-31.

15. Ter Minassian-Saraga, L. (1956). *Recent work on spread monolayers, adsorption and desorption*. *Journal of Colloid Science* 11.4: 398-418.

16. Zaidan, Shatha (2020). *Effect of obesity on blood-brain barrier integrity in ischemic brain using mouse model*. Ph. D. dissertation, University of Saarland, doi:10.22028/D291-31218.

17. Wong, B.X., Hung, Y.H., Bush, A.I. and Duce, J.A. (2014). *Metals and cholesterol: two sides of the same coin in Alzheimer's disease pathology*. Frontiers in aging neurosciences. vol. **6** Article 91, 12.

18. Bulloj, A., Maria C. Leal, Surace, E.I., Zhang, X., Huaxi, X., Maria D. Ledesma, Castano, E.M., and Laura Morelli. (2008). *Detergent resistant membrane-associated IDE in brain tissue and cultured cells: relevance to Aβ and insulin degradation.* Molecular neurodegeneration, 3:22.

19. Saido, T. and Leissring, M.A. (2012). *Proteolytic degradation of amyloid β-protein*. Cold Spring Harb Perspect Mec **2**: a006379.

20. Qiu, W.Q., Walsh, D.M., Zhen, Y., Vekrellis, K., Jimin, Z., Podlisny, M.P., Rosner, M.R., Afshin, S. and Hersh. L.B. (1998). *Insulin-degrading enzyme regulate extracellular levels of amyloid β-protein by degradation*. The journal of Biological Chemistry, vol. 273, No. **49**, pp. 8 32730-32738.

21. Grimm, M.O., Haupenthal, V.J., Rothhaar, T.L., Zimmer, V.C., Grosgen, S., Hudsdorfer, B., Lehmann, J., Grimm, H.S., and Hartmann, T. (2013). *Effect of different phospholipids on alphs-secretase activity in the non-amyloidogenic pathway of Alzheimer's disease*. International journal of molecular sciences **14**, 5879-5898.
22. Dietschy J.M. and Stephen D.T. (2004). *Cholesterol metabolism in the central nervous system during development and in the mature animal*. Journal of lipid research Volume 45.
23. Dietschy, J.M. (2009). *Central nervous system: cholesterol turnover, brain development and neurodegeneration*. Biol. Chem; **390**(4): 287-293.
24. Bjorkhem, I. (2006). *Crossing the barrier: oxysterols as cholesterol transporters and metabolic modulators in the brain*. J. of Internal Med. 260 :493-508.
25. Petrov, A. M., Kasimov, M. R., and Zefirov, A. L. (2016). *Brain cholesterol metabolism and its defects: Linkage to neurodegenerative diseases and synaptic dysfunction*. Park- media Ltd. ACTA nature, Vol. 8, No. 1 (28).
26. Fantini, J., Di Scala, C., Evans, L. S., Williamson, P. T. F., and, Barrantes, F. J. (2016). *A mirror code for protein cholesterol interactions in the two leaflets of biological membranes. Scientific reports*, 6:21907 DOI: 10.1038/srep21907
27. Fantini, J., Yahi, N., and Garmy, N. (2013). *Cholesterol accelerates the binding of Alzheimer's β-amyloid peptide to ganglioside GM1 through a universal hydrogen-bond-dependent sterol tuning of glycolipid conformation*. Frontiers in physiology, June 2013 | Volume 4 | Article 120, doi: 10.3389/fphys.2013.00120
28. Di Scala, C., Fantini, J., Yahi, N., Barrantes, F. J., and Chahinian, H. (2018). *Anandamide Revisited: How Cholesterol and Ceramides Control Receptor-Dependent and Receptor-Independent Signal Transmission Pathways of a Lipid Neurotransmitter*. Biomolecules 2018, 8, 31; doi:10.3390/biom8020031
29. Baier, C. J., Fantini, J., and Barrantes, F. J. (2011). *Disclosure of cholesterol recognition motifs in transmembrane domains of the human nicotinic acetylcholine receptor*. SCIENTIFIC REPORTS | 1 : 69 | DOI: 10.1038/srep00069
30. Grimm, M.O., Mett, J., Stahlmann, C.P., Grosgen, S., Haupenthal, V.J., Blumel, T., Hundsdorfer, B., Zimmer, V.C., Mylonas, N.T., Tanila, H., et al. (2015). *APP intracellular domain derived from amyloidogenic β- and γ-secretase cleavage regulates neprilysin expression.* Front. Aging Neurosci. **7**, 77-94.
31. Weller, R.O., Massey, A., Yu-Min, K. and Roher, A.E. (2000). *Cerebral amyloid angiopathy: accumulation of Aβ in interstitial fluid drainage pathways in Alzheimer's disease*. Cerebral amyloid angiopathy, 903:110-7.
32. Zhao, J., Li, L., and Leissring, M.A. (2009). *Insulin-degrading enzyme is exported via an unconventional protein secretion pathway.* BioMed Central, Molecular Neurodegeneration, 4:4 doi:10.1186/1750-1326-4-4.
33. Song, E.S., Rodgers, D.W. and Hersh, L.B. (2018). *Insulin-degrading enzyme is not secreted from cultured cells.* Scientific Reports, 8:2335, doi:10.10:38/s41598-018-20597-6.
34. Steffen, J., Krohn, M., Schwitlick, C., Btuening, T., Paarmann, K., Pietrzik, C. U., Biverstal, H., Jansone, B., Langer, O., and Pahnke, J. (2017). *Expression of endogenous mouse APP modulates β-amyloid deposition in hAPP-transgenic mice.* Acta neuropathological communications 5:49

35. Bright, J., Hussain, S., Dang, V., Wright, S., Cooper, B., Byun, T., Ramos, C., Singh, A., Parry, G., Stagliano, N., and Prenner, I. G., (2015). *Human secreted tau increases amyloid-beta production.* Neurobiology of aging 36, 693-709.
36. Fung, J., Frost, D., Chakrabartty, A., and McLaurin, J., (2004). *Interaction of human and mouse Aβ peptides.* Journal of neurochemistry, doi: 10.1111/j.1471-4159.2004.02828.x.